

Electronic Supplementary Information

On the coordination chemistry of phosphinecarboxamide:

Assessing ligand basicity

Michael B. Geeson, Andrew R. Jupp, John E. McGrady and Jose M. Goicoechea*

Department of Chemistry, University of Oxford, Inorganic Chemistry Laboratory, South

Parks Road, Oxford, OX1 3QR, U.K.

CONTENTS

1. Experimental section
2. Computational data
3. NMR spectra
4. IR spectra
5. References

1. Experimental section

1.1. General synthetic considerations

All reactions and product manipulations were carried out under an inert atmosphere of argon or dinitrogen using standard Schlenk or glovebox techniques (MBraun UNILab glovebox maintained at $<0.1\text{ppm O}_2$ and $<0.1\text{ppm H}_2\text{O}$) unless otherwise specified.

Dichloromethane (CH_2Cl_2 ; Sigma Aldrich, HPLC grade), hexane (hex; Sigma Aldrich, HPLC grade), pentane (pent; Sigma Aldrich, HPLC grade) and toluene (tol; Sigma Aldrich, HPLC grade) were purified using an MBraun SPS-800 solvent system. d_8 -THF ($>99.5\%$; Euristop) and CD_2Cl_2 ($>99.5\%$, Euristop) were dried over CaH_2 , vacuum distilled, and degassed before

use. All dry solvents were stored under argon in gas-tight ampoules. Additionally dichloromethane, hexane, pentane, THF and toluene were stored over activated 3 Å molecular sieves. Deionised water was obtained from a Millipore Milli-Q purification system. Ammonia (anhydrous, BOC) was used as received. Ammonium tetraphenylborate (99%; Sigma Aldrich), 1,5-cyclooctadiene (99%; Sigma Aldrich), tungsten hexacarbonyl (99%; Strem Chemicals) and molybdenum hexacarbonyl (98%; Acros Organics) were used as received without any further purification. $[\text{Na}(\text{dioxane})_{1.75}][\text{PCO}]$,¹ $[\text{K}(18\text{-crown-6})][\text{PCO}]$,² and $\text{Mo}(\text{CO})_4(\text{COD})$ ³ were prepared according to literature methods and stored at ambient temperature in an inert atmosphere glovebox. $\text{PH}_2\text{C}(\text{O})\text{NH}_2$ was prepared via a modified procedure previously reported by our research group (*vide infra*).⁴

1.2. Synthesis

Synthesis of $\text{PH}_2\text{C}(\text{O})\text{NH}_2$. $[\text{Na}(\text{dioxane})_{1.75}][\text{PCO}]$ (12.75g, 54.0 mmol) and $[\text{NH}_4][\text{BF}_4]$ (5.66g, 54.0 mmol) were added to a Schlenk flask in an inert atmosphere glovebox. Ammonia (approx. 50 mL) was condensed into the flask at $-78\text{ }^\circ\text{C}$ and the resulting pale yellow solution was stirred for one hour, after which it was allowed to slowly warm to room temperature under a flow of argon. Dioxane was removed from the solid under dynamic vacuum at $15\text{ }^\circ\text{C}$ to minimise product loss. $\text{PH}_2\text{C}(\text{O})\text{NH}_2$ was isolated as colourless crystals by sublimation, at 2×10^{-2} mbar and $50\text{ }^\circ\text{C}$. Yield 1.55g (37%). m.p. = $64\text{ }^\circ\text{C}$. The product was stored at $-25\text{ }^\circ\text{C}$ in an inert atmosphere glovebox with the exclusion of light. Spectroscopic data for the product are consistent with previously reported values.⁴

*Synthesis of $[\text{W}(\text{PH}_2\text{C}(\text{O})\text{NH}_2)(\text{CO})_5]$ (**1**).* A d_8 -THF (0.5 mL) solution of $\text{PH}_2\text{C}(\text{O})\text{NH}_2$ was prepared from $[\text{K}(18\text{-crown-6})][\text{PCO}]$ (55.8 mg, 0.150 mmol) and $[\text{NH}_4][\text{B}(\text{C}_6\text{H}_5)_4]$ (52.0 mg, 0.150 mmol) in a NMR tube equipped with a gas-tight tap. $\text{W}(\text{CO})_6$ (32 mg, 0.090

mmol) was dissolved in d_8 -THF (1 mL) and transferred to an ampoule equipped with a gas-tight tap. The ampoule was degassed via the freeze-pump-thaw method. The solution was stirred under a mercury lamp (150W) for one hour to afford a bright yellow solution. The atmosphere was replaced with argon, and the solution cooled to -78 °C to precipitate unreacted $W(CO)_6$. The bright yellow solution was transferred to the NMR tube containing the d_8 -THF solution of phosphinecarboxamide and monitored by NMR spectroscopy. Crystallisation was attempted by layering the THF solution with an antisolvent (hex, pent, tol), slow evaporation from a concentrated THF solution and cooling a concentrated THF solution to -86 °C in a freezer. 1H NMR (500 MHz, d_8 -THF, 298K): δ (ppm) 7.63 (b, s, 1H; NH), 7.40 (m, 1H; NH), 5.22 (d, $^1J_{P-H} = 347$ Hz, 2H; PH_2). ^{31}P NMR (202.4 MHz, d_8 -THF, 298K): δ (ppm) -103.1 (td, $^1J_{P-H} = 347$, $^3J_{P-H} = 21$ Hz, sat. $^1J_{W-P} = 216$ Hz). $^{31}P\{^1H\}$ NMR (202.4 MHz, d_8 -THF, 298K): δ (ppm) -103.1 (s, sat. $^1J_{W-P} = 216$ Hz). $^{13}C\{^1H\}$ NMR (125.8 MHz, d_8 -THF, 298K): δ (ppm) 196.2 (d, $^2J_{C-P} = 7$ Hz, sat. $^1J_{W-C} = 126$ Hz; *trans*-CO), 192.5 (s, sat. $^1J_{W-P} = 127$ Hz; *cis*-CO), 168.4 (d, $^1J_{C-P} = 54$ Hz; $PH_2C(O)NH_2$). IR (THF solution): ν (cm^{-1}) 2077 (CO stretch), 1968 (CO stretch), 1926 (CO stretch), 1882 (CO), 1645 ($PH_2(CO)NH_2$ stretch).

Synthesis of $[Mo(PH_2C(O)NH_2)_2(CO)_4]$ (2). $PH_2C(O)NH_2$ (100 mg, 1.30 mmol) and $Mo(CO)_4(COD)$ (205 mg, 0.65 mmol) were weighed out under an inert atmosphere, dissolved in CH_2Cl_2 (3 mL) and transferred to an ampoule equipped with a gas-tight tap. The solution was stirred overnight to afford a pale yellow precipitate and a red oil. The pale precipitate was dissolved in a further 10 mL of CH_2Cl_2 and separated from the red oil by filtration. The pale yellow filtrate was washed with CH_2Cl_2 (3×5 mL) to remove COD and dried under dynamic vacuum for a further four hours to recover a pale yellow powder. Yield 63 mg (17.4%). Anal. Calcd for $MoC_6O_6N_2P_2H_8$: C: 19.90; H: 2.23; N: 7.74. Found C: 20.12;

H: 2.38; N: 7.48. ^1H NMR (500.0 MHz, CD_2Cl_2 , 298K): δ (ppm) 6.71 (br, s, 1H; NH), 5.92 (br, d, 1H; NH), 5.00 (m, $^1J_{\text{P-H}} = 328$ Hz, $^3J_{\text{P-H}} = 9$ Hz, 2H; PH_2). $^1\text{H}\{^{31}\text{P}\}$ NMR (500.0 MHz, CD_2Cl_2 , 298K): δ (ppm) 5.00 (s, 2H; PH_2), the rest of the resonances are observed as detailed above. ^{31}P NMR (202.4 MHz, CD_2Cl_2 , 298K): δ (ppm) -64.9 (m, $^1J_{\text{P-H}} = 328$ Hz, $^2J_{\text{P-P}} = -25$ Hz, $^3J_{\text{P-H}} = 18$ Hz, $^3J_{\text{P-H}} = 9$ Hz). $^{31}\text{P}\{^1\text{H}\}$ NMR (202.4 MHz, CD_2Cl_2 , 298K): δ (ppm) -64.9 (s). $^{13}\text{C}\{^1\text{H}\}$ NMR (125.8 MHz, CD_2Cl_2 , 298K): δ (ppm) 212.1 (m; *cis*-CO), 206.8 (t, $^2J_{\text{C-P}} = 9$ Hz; *trans*-CO), 171.9 (m, $\text{PH}_2\text{C}(\text{O})\text{NH}_2$). CCDC 1014321 contains the supplementary crystallographic data. IR (Nujol mull): ν (cm^{-1}) 2040 (CO stretch), 1930 (CO stretch), 1886 (CO stretch), 1639 ($\text{PH}_2(\text{CO})\text{NH}_2$ stretch).

1.3. Characterisation Techniques

1.3.1 NMR spectroscopy

^1H , $^{13}\text{C}\{^1\text{H}\}$, and ^{31}P NMR spectra were acquired at 500.0, 125.8 and 202.4 MHz, respectively, on a Bruker AVIII 500 MHz NMR spectrometer. ^1H and ^{13}C spectra are reported relative to $\text{Si}(\text{CH}_3)_4$ ($\delta_{\text{H}} = 0$ ppm, $\delta_{\text{C}} = 0$ ppm) and were referenced to the most downfield residual solvent resonance (*d*₈-THF: $\delta_{\text{H}} = 3.58$ ppm, $\delta_{\text{C}} = 67.57$ ppm; CD_2Cl_2 : $\delta_{\text{H}} = 5.32$ ppm, $\delta_{\text{C}} = 53.8$ ppm). ^{31}P spectra were externally referenced to 85% H_3PO_4 ($\delta_{\text{P}} = 0$ ppm). All spectra were obtained at 25 °C. Spectral simulations were carried out using the gNMR v5.0 program. Data were processed using the Bruker TopSpin 3.1 program.⁵

1.3.2 Single crystal X-ray structure determination

Single-crystal X-ray diffraction data were collected using an Oxford Diffraction Supernova dual-source diffractometer equipped with a 135 mm Atlas CCD area detector. Crystals were selected under Paratone-N oil, mounted on micromount loops, and quench-cooled using an Oxford Cryosystems open flow N_2 cooling device.⁶ Data were collected at 150 K using

mirror monochromated Cu K α radiation ($\lambda = 1.5418 \text{ \AA}$) and processed using the CrysAlisPro package, including unit cell parameter refinement and interframe scaling (which was carried out using SCALE3 ABSPACK within CrysAlisPro).⁷ Equivalent reflections were merged and diffraction patterns processed with the CrysAlisPro suite. Structures were subsequently solved using direct methods, and refined on F^2 using the SHELXL-2014.⁸

1.3.3 IR spectroscopy

IR data were recorded in a THF solution (**1**) or as a solid sample in a Nujol mull (**2**). Both were prepared inside an inert atmosphere glovebox and the samples placed in an airtight holders prior to data collection. Spectra were recorded on a Thermo Scientific iS5 FT-IR spectrometer in absorbance mode.

2. Computational data

2.1 Computational details

All density functional theory calculations were performed using the ADF2013.01 software package.⁹ The BP86 functional was used throughout,¹⁰ along with the D3-bj damped dispersion correction.¹¹ Relativistic effects were included at the scalar ZORA level.¹² A triple-zeta + polarisation quality basis of Slater-type orbitals was used on all atoms. The nature of stationary points was confirmed by frequency analysis: in all cases all frequencies were real. All quantum chemical results were visualised using the Chemcraft 1.7 software.¹³

NMR properties of $\text{Mo}(\text{CO})_4(\text{PH}_2\text{C}(\text{O})\text{NH}_2)_2$ were calculated with the ADF package.⁹ The local density approximation (LDA) of Perdew and Wang's 1992 functional (PW92) was used with a generalised gradient approximation (GGA) through the exchange and correlation

functionals of Perdew, Burke and Ernzerhof (PBE).^{14,15} An all electron QZ4P basis sets were used on all atoms and no frozen core approximations were used.

Fragment calculations were performed by first converging separate single point calculations for the $W(CO)_5$ and PR_3 units in the geometries they adopt in the optimised structure of $W(CO)_5(PR_3)$. The complete molecule is then reassembled using the converged orbitals of the fragments as a basis: in this way, the resulting total energy, ΔE_{tot} , reflects the energy of the W–P bond in isolation. ΔE_{tot} can be decomposed into the sum of three components, the steric energy, ΔE_{steric} , a dispersion contribution, ΔE_{disp} , and an orbital interaction term, ΔE_{oi} . The steric term arises through the orthogonalisation of the orbitals on the fragments before electron density is allowed to redistribute into their vacant orbitals. The ΔE_{oi} term relates to the stabilisation gained from allowing the electron density to relax through charge transfer from the occupied orbitals of one fragment to the vacant orbitals of the other. The fragment calculation can also be performed after removing some or all of the vacant orbitals on either of the two fragments ($W(CO)_5$ or PR_3). In the present case, if all the vacant orbitals on PR_3 are removed, back-bonding into the PR_3 fragment is effectively blocked. Conversely, if the vacant orbitals on $W(CO)_5$ are removed, σ -donation from the PR_3 unit is blocked. The changes in the ΔE_{oi} term induced by removing various subsets of orbitals therefore provide a measure of the relative contributions of forward- and back-bonding to the total interaction energies.

These results of these fragment calculations on $W(CO)_5(PR_3)$ are summarised in Table S1. In terms of the analysis of forward and back-bonding, the key terms are the total orbital interaction energy, ΔE_{oi} , and the corresponding values when the vacant orbitals on PR_3 and on $W(CO)_5$ are removed (bottom three rows of the table). The difference in ΔE_{oi} with and

without the vacant orbitals on PR_3 is a measure of the contribution of back-bonding to the total bond strength: for PH_3 this is 18.7 kcal/mol ($= -49.6 - (-30.9)$), which equates to 38% of the total orbital interaction energy ($100 \times 18.7/49.6$). The corresponding numbers for $\text{PH}_2\text{C}(\text{O})\text{NH}_2$, PMe_3 and PF_3 are 38% ($100 \times 20.6/54.6$), 33% ($100 \times 20.0/54.2$) and 44% ($100 \times 27.8/63.7$), respectively. Conversely, the difference in ΔE_{oi} with and without the vacant orbitals on $\text{W}(\text{CO})_5$ is a measure of the relative importance of $\text{P} \rightarrow \text{W}$ σ donation. The corresponding numbers are: PMe_3 , 60% ($= 100 \times (-49.6 - (-22.2)) / -49.6$); PH_3 , 55%; $\text{PH}_2(\text{CO})\text{NH}_2$, 55%; PF_3 , 45%. Note that the contributions from forward- and back-bonding sum to slightly less than 100%: this is because even in the absence of vacant orbitals on PR_3 , the presence of occupied orbitals on this fragment allows the orbitals on $\text{W}(\text{CO})_5$ to relax, effectively redistributing electron density between occupied and virtual spaces on the same fragment.

The overall picture that emerges from this analysis is therefore that $\text{PH}_2\text{C}(\text{O})\text{NH}_2$ bears a striking similarity to PH_3 , in so much as it is a moderate σ -donor and π -acceptor, consistent with the available spectroscopic evidence.

Table S1. Fragment decomposition of the interaction energy between $W(CO)_5$ and PR_3 fragments (distances in Å, energies in kcal/mol).

	PMe₃	PH₃	PH₂C(O)NH₂	PF₃
Distances				
Mo–P	2.52	2.50	2.50	2.40
Mo–CO (<i>cis</i>)	2.05	2.06	2.04	2.06
Mo–CO (<i>trans</i>)	2.03	2.02	2.03	2.05
Energies				
$\Delta E_{\text{tot}} (= \Delta E_{\text{steric}} + \Delta E_{\text{disp}} + \Delta E_{\text{oi}})$	-62.0	-44.7	-50.5	-45.9
ΔE_{steric}	6.8	13.1	15.4	26.8
ΔE_{disp}	-14.6	-8.2	-11.4	-9.0
ΔE_{oi}	-54.2	-49.6	-54.6	-63.7
$\Delta E_{\text{oi}}(-PR_3 \text{ virtuals})$	-36.2	-30.9	-34.0	-35.9
$\Delta E_{\text{oi}}(-W(CO)_5 \text{ virtuals})$	-21.7	-22.2	-24.5	-35.3

Cartesian coordinates (in Å) and total energies (in eV) of all stationary points.

(1) $W(CO)_5(PH_3)$. -105.282 eV.

1. W	-0.002202	0.007836	2.466952
2. O	-3.218752	0.008027	2.440658
3. O	-0.001329	3.224649	2.432416
4. O	3.214844	0.008208	2.428499
5. O	-0.001468	-3.209018	2.441465
6. O	0.005645	0.010857	5.653348
7. C	0.002078	0.010330	4.491825
8. C	-2.058927	0.008243	2.457458
9. C	-0.001971	2.064777	2.448766
10. C	2.054692	0.008171	2.442671
11. C	-0.002095	-2.048937	2.453293
12. P	0.013582	-0.004402	-0.036086
13. H	0.762782	-0.993379	-0.736789
14. H	-1.199588	-0.158334	-0.767569
15. H	0.505932	1.122815	-0.755331

(2) W(CO)₅(PMe₃). -155.583 eV.

1. W	-0.001384	0.013422	2.462167
2. O	-3.215440	0.040149	2.385791
3. O	-0.010521	3.228907	2.420075
4. O	3.212663	0.057075	2.397784
5. O	0.004490	-3.197386	2.315384
6. O	-0.003642	-0.029805	5.655741
7. C	-0.003949	-0.010033	4.493056
8. C	-2.053828	0.025675	2.424055
9. C	-0.007096	2.067055	2.446485
10. C	2.050744	0.035811	2.432039
11. C	0.003026	-2.036460	2.387181
12. P	0.005822	-0.027484	-0.056177
13. H	1.348309	-0.892073	-1.927124
14. H	-1.481689	-1.907373	-0.476828
15. H	0.027602	1.471167	-2.007702
16. C	0.025157	1.600683	-0.916048
17. H	-0.859319	2.179506	-0.617138
18. H	0.921337	2.158490	-0.611603
19. C	1.432258	-0.897433	-0.831187
20. H	2.366506	-0.403482	-0.531681
21. H	1.459767	-1.934914	-0.470402
22. C	-1.430828	-0.871883	-0.840617
23. H	-2.357691	-0.358677	-0.550575
24. H	-1.337933	-0.871433	-1.935859

(3) W(CO)₅(PF₃). -109.608 eV.

1. W	-0.006635	0.006335	2.434036
2. O	-3.225060	0.010223	2.518021
3. O	-0.011768	3.225786	2.477356
4. O	3.212590	0.009017	2.453658
5. O	-0.013332	-3.212172	2.493716
6. O	0.028085	0.012317	5.637353
7. C	0.013399	0.011306	4.480929
8. C	-2.070053	0.008045	2.478174
9. C	-0.008871	2.069974	2.451929
10. C	2.056121	0.007160	2.435176
11. C	-0.009796	-2.056414	2.461100
12. P	0.007180	-0.013240	0.036361
13. F	0.913424	-1.084659	-0.721869
14. F	-1.345398	-0.265666	-0.770436
15. F	0.494296	1.281174	-0.757898

(4) W(CO)₅(PH₂CONH₂) (1). -133.164 eV.

1. W	0.041479	-0.354605	1.267538
2. P	0.092865	-0.561067	-1.225365

3. H	-0.609218	-1.629904	-1.844567
4. H	1.334668	-0.753145	-1.897115
5. O	-0.908957	0.447381	-3.568826
6. C	-0.576885	0.772772	-2.438592
7. N	-0.609684	2.029592	-1.938250
8. H	-0.944850	2.783539	-2.532284
9. H	-0.360287	2.233077	-0.97589
10. C	-0.292209	-2.388599	1.378549
11. O	-0.119749	-0.205302	4.450703
12. C	-1.985178	-0.027343	1.115186
13. O	0.540264	2.811834	1.138637
14. C	0.373836	1.659064	1.200464
15. O	3.218606	-0.848085	1.368261
16. C	2.072822	-0.676689	1.337949
17. O	-0.474627	-3.528923	1.461460
18. C	-0.055974	-0.258430	3.292772
19. O	-3.124998	0.158078	1.009753

(5) Mo(CO)₄(PH₂CONH₂)₂ (2). -160.455 eV.

1. Mo	0.000000	0.000000	-1.823360
2. P	0.820183	1.736687	-0.210562
3. H	2.178506	2.145172	-0.379774
4. H	0.243034	3.034287	-0.160822
5. C	0.838026	1.471039	1.676616
6. O	0.072847	2.086866	2.413053
7. N	1.726690	0.528864	2.095043
8. H	1.586039	0.138707	3.026064
9. H	2.138908	-0.100789	1.411258
10. P	-0.820183	-1.736687	-0.210562
11. H	-2.178506	-2.145172	-0.379774
12. H	-0.243034	-3.034287	-0.160822
13. C	-0.838026	-1.471039	1.676616
14. O	-0.072847	-2.086866	2.413053
15. N	-1.726690	-0.528864	2.095043
16. H	-1.586039	-0.138707	3.026064
17. H	-2.138908	0.100789	1.411258
18. C	1.894000	-0.814374	-1.789436
19. O	2.972283	-1.247409	-1.761801
20. C	0.583988	1.311872	-3.253221
21. O	0.926896	2.066340	-4.069603
22. C	-1.894000	0.814374	-1.789436
23. O	-2.972283	1.247409	-1.761801
24. C	-0.583988	-1.311872	-3.253221
25. O	-0.926896	-2.066340	-4.069603

2.2 Computed structural parameters for **1**

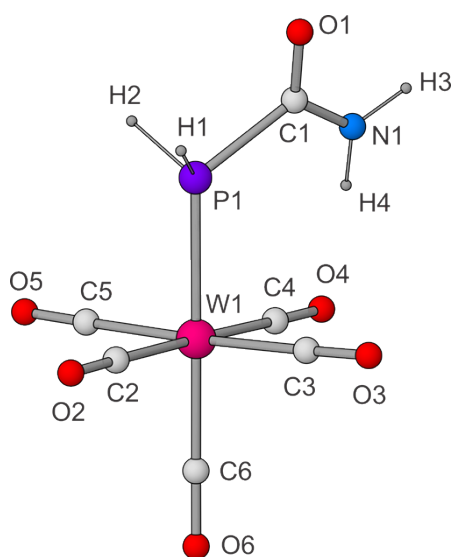


Table S2. Interatomic bond distances (Å) for the optimized computed geometries of **1**.

Distance	I_{calc}
W1–P1	2.50
W1–C2	2.06
W1–C3	2.06
W1–C4	2.04
W1–C5	2.06
W1–C6	2.03
P1–C1	1.92
C1–O1	1.22
C1–N1	1.35
C2–O2	1.16
C3–O3	1.16
C4–O4	1.17
C5–O5	1.16
C6–O6	1.16
P1–H1	1.42
P1–H2	1.42
N1–H3	1.02
N1–H4	1.01

2.3 Computed structural parameters for **2**

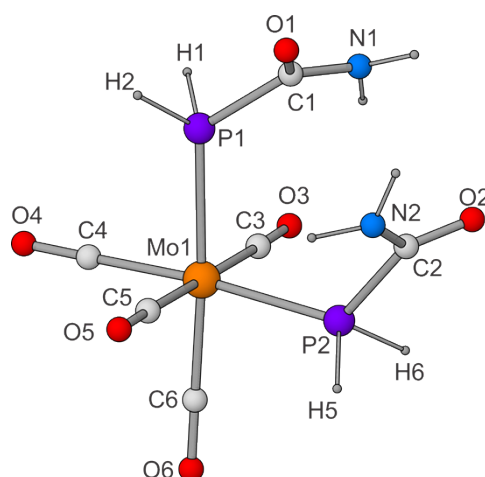


Table S3. Interatomic bond distances (Å) for the crystallographically characterized and optimized computed geometries of **2**.

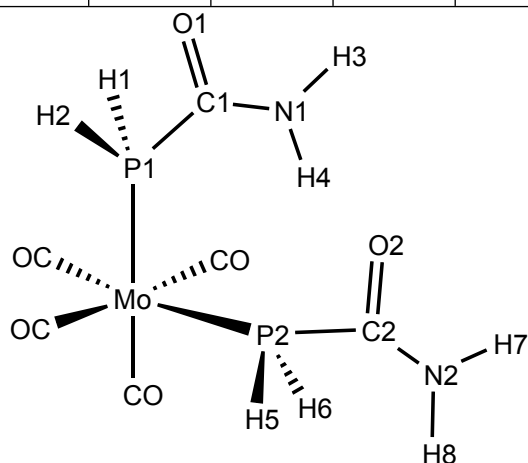
	z_{exp}	z_{calc}
Mo1–P1	2.481(1)	2.51
Mo1–P2	2.480(1)	2.51
Mo1–C3	2.044(2)	2.06
Mo1–C4	1.997(2)	2.03
Mo1–C5	2.041(2)	2.06
Mo1–C6	1.995(2)	2.03
P1–C1	1.870(2)	1.91
C1–O1	1.230(2)	1.23
C1–N1	1.325(2)	1.36
P2–C2	1.871(2)	1.91
C2–O2	1.226(2)	1.23
C2–N2	1.328(2)	1.36
C3–O3	1.140(2)	1.16
C4–O4	1.147(2)	1.16
C5–O5	1.140(2)	1.16
C6–O6	1.148(2)	1.16
P1–H1	1.32(3)	1.42
P1–H2	1.27(2)	1.43
P2–H5	1.25(2)	1.43
P2–H6	1.28(2)	1.42

Table S4. Interatomic bond angles (°) for the crystallographically characterized and optimized computed geometries of **2**.

	α_{exp}	α_{calc}
P1–Mo1–P2	91.73(1)	99.96
P1–Mo1–C3	86.56(4)	87.85
P1–Mo1–C4	92.49(5)	84.91
P1–Mo1–C5	87.60(4)	90.94
P2–Mo1–C3	89.47(4)	90.94
P2–Mo1–C5	85.33(4)	87.85
P2–Mo1–C6	91.62(5)	84.91
C3–Mo1–C4	94.27(6)	90.15
C3–Mo1–C6	91.60(6)	91.18
C4–Mo1–C5	91.35(6)	91.18
C4–Mo1–C6	84.28(7)	90.25
C5–Mo1–C6	94.54(6)	90.15
Mo1–P1–C1	117.43(5)	122.91
P1–C1–O1	118.0(1)	121.22
P1–C1–N1	118.0(1)	114.02
O1–C1–N1	124.0(2)	124.74
Mo1–P2–C2	118.27(5)	122.91
P2–C2–O2	118.3(1)	121.22
P2–C2–N2	117.8(1)	114.02
O2–C2–N2	123.9(2)	124.74
H1–P1–H2	100(2)	97.43
H5–P2–H6	98(1)	97.43

Table S5. Simulated and computed (in brackets) coupling constants (Hz) for **2** (numbering scheme pictured below).

	P1	P2	H1	H2	H5	H6	H3	H4	H7	H8
P1		-24.9 (-9.6)	328.2 (248.6)	328.2 (309.8)	8.6 (2.2)	8.6 (4.6)	17.8 (14.5)			
P2	-24.9 (-9.6)		8.6 (4.6)	8.6 (2.3)	328.2 (310.9)	328.2 (253.6)			17.8 (14.6)	
H1	328.2 (248.6)	8.6 (4.6)								
H2	328.2 (309.8)	8.6 (2.3)								
H5	8.6 (2.2)	328.2 (310.9)								
H6	8.6 (4.6)	328.2 (253.6)								
H3	17.8 (14.5)									
H4										
H7		17.8 (14.6)								
H8										



3. NMR spectra

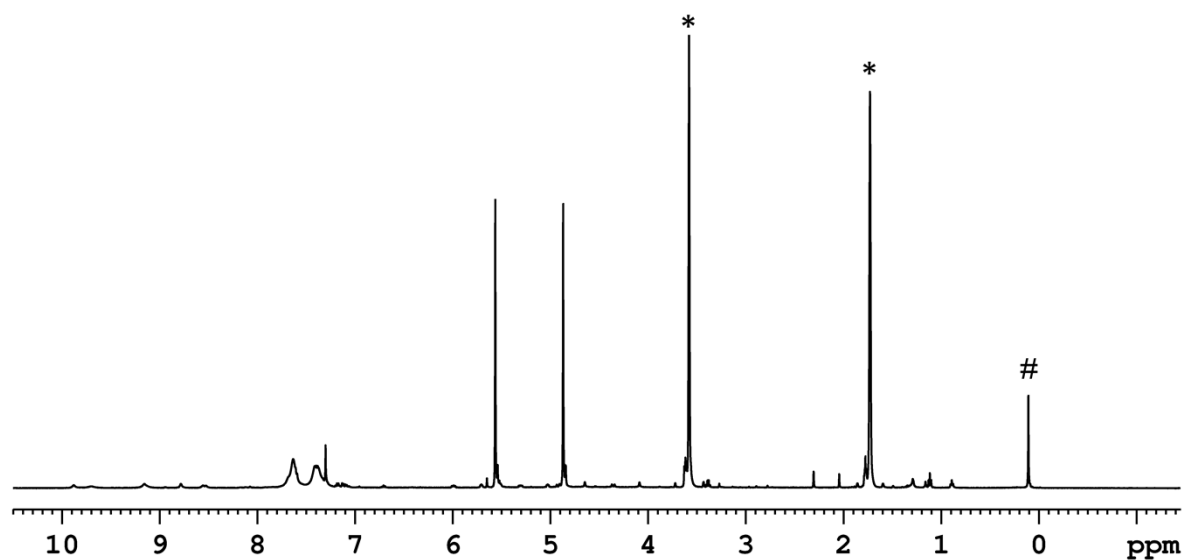


Figure S1. ^1H NMR spectrum of **1** in d_8 -THF. The resonances marked with * are due to the solvent, and # is due to a grease impurity.

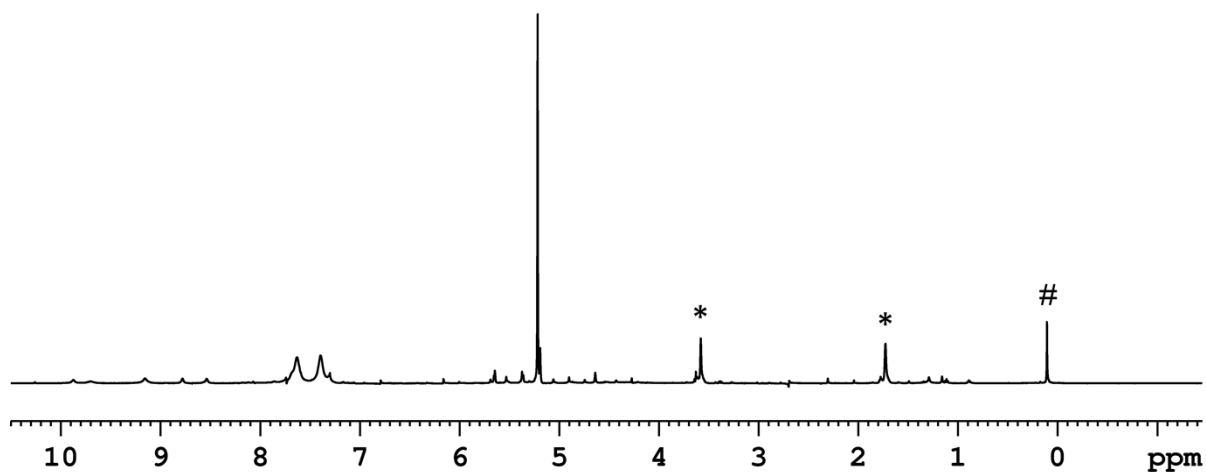


Figure S2. $^1\text{H}\{^{31}\text{P}\}$ NMR spectrum of **1** in d_8 -THF. The resonances marked with * are to the solvent, and # is due to a grease impurity.

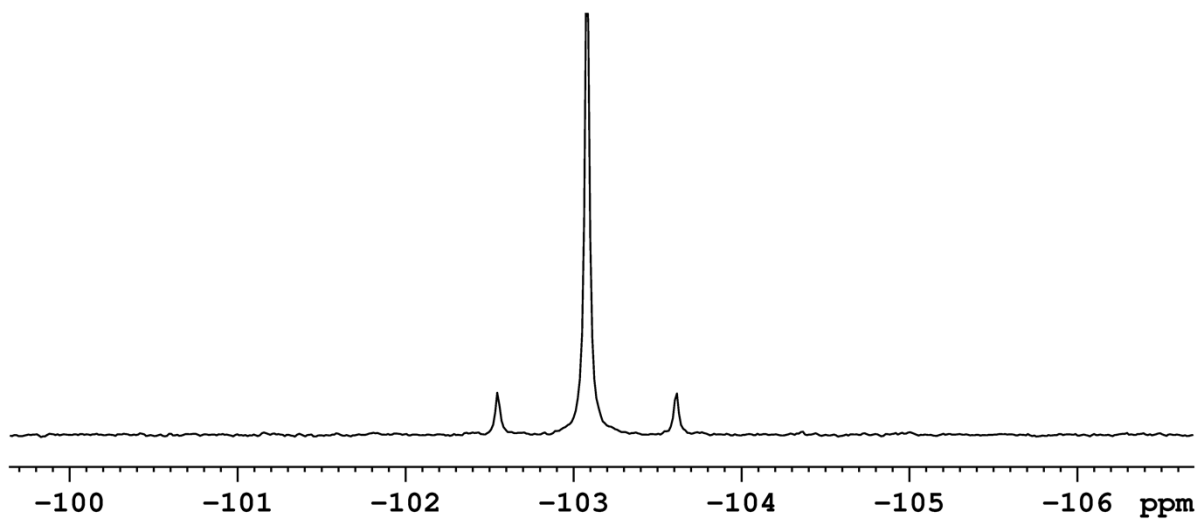


Figure S3. $^{31}\text{P}\{^1\text{H}\}$ NMR spectrum of **1** in d_8 -THF.

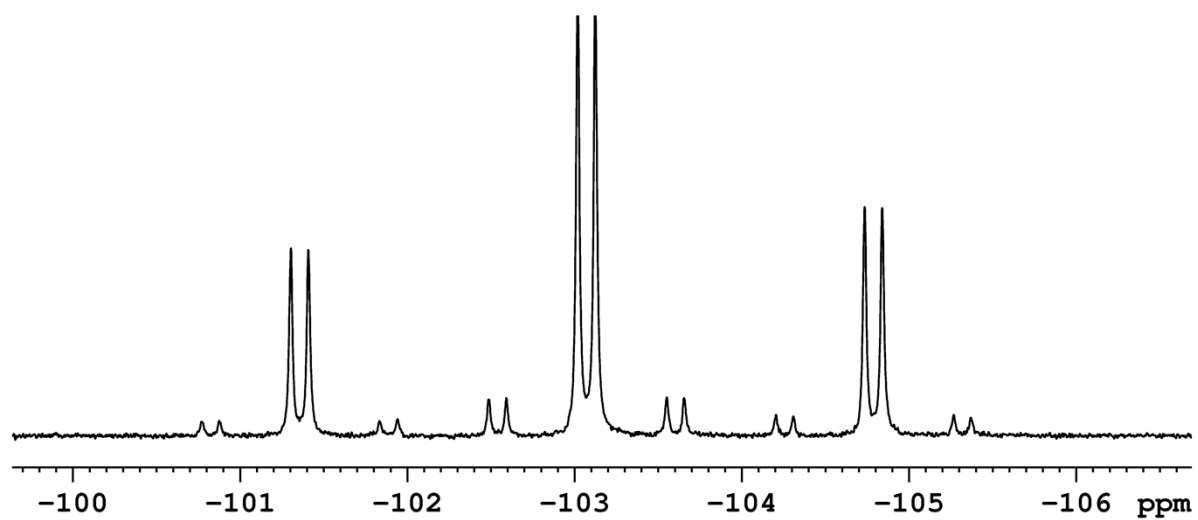


Figure S4. ^{31}P NMR spectrum of **1** in d_8 -THF.

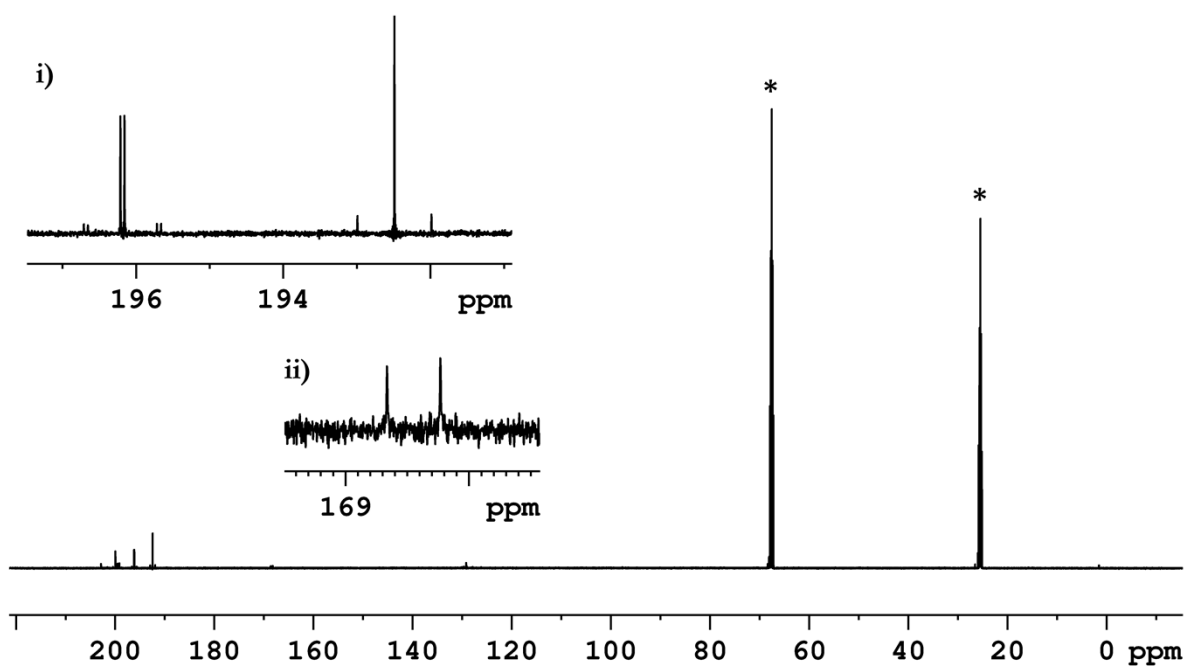


Figure S5. $^{13}\text{C}\{^1\text{H}\}$ NMR spectrum of **1** in d_8 -THF. Resonances marked with * are to the solvent. Inset i) shows the zoomed in region for the *trans* and *cis* carbonyls, and inset ii) shows the phosphinecarboxamide resonance.

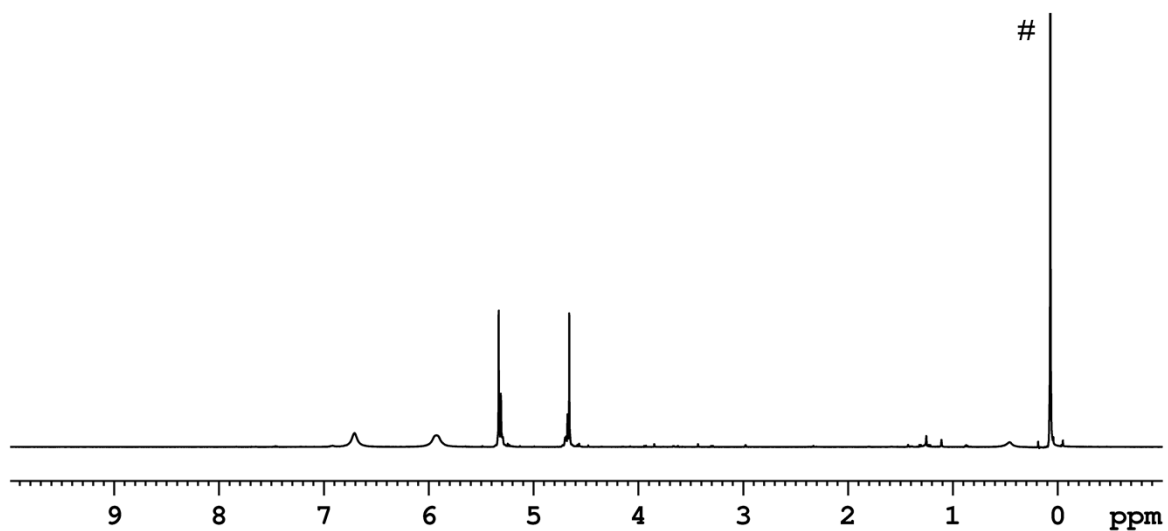


Figure S6. ^1H NMR spectrum of **2** in CD_2Cl_2 . The solvent resonance is obscured by the product. The resonance marked with # is due to a grease impurity.

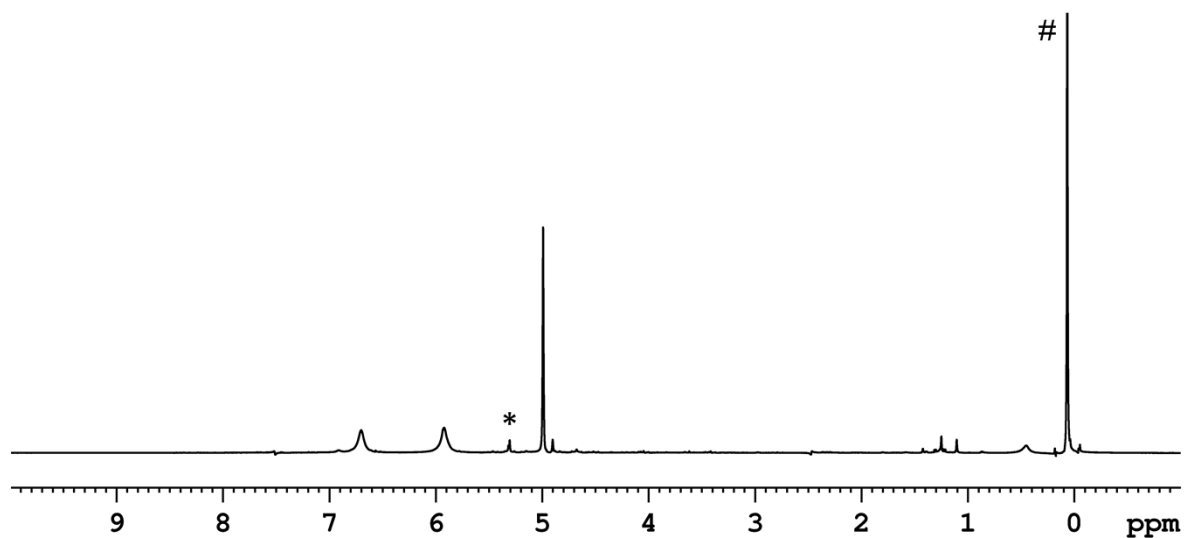


Figure S7. $^1\text{H}\{^{31}\text{P}\}$ NMR spectrum of **2** in CD_2Cl_2 . The resonance marked with * is to the solvent, and # is due to a grease impurity.

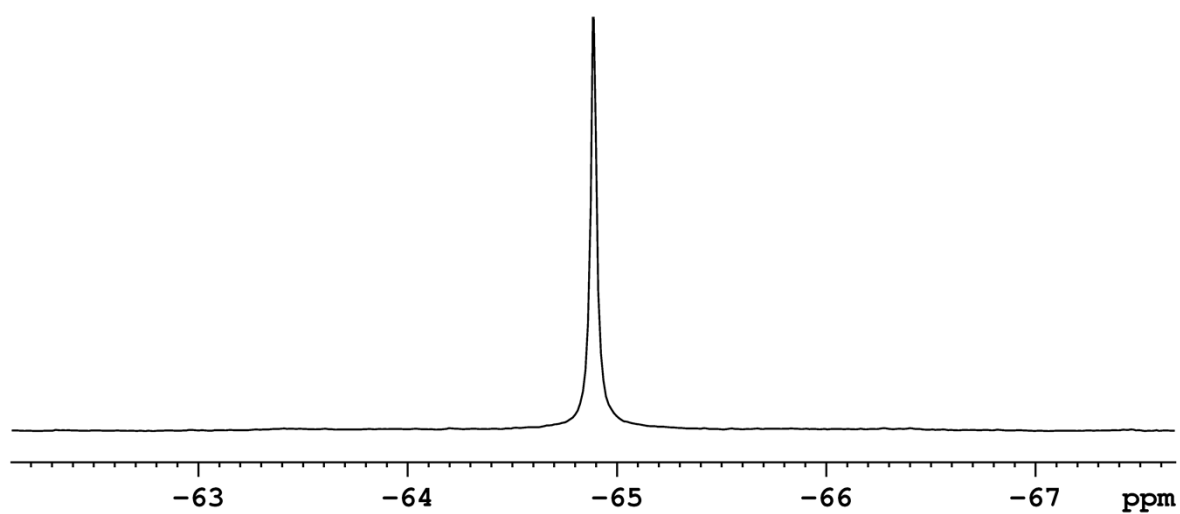


Figure S8. $^{31}\text{P}\{^1\text{H}\}$ NMR spectrum of **2** in CD_2Cl_2 .

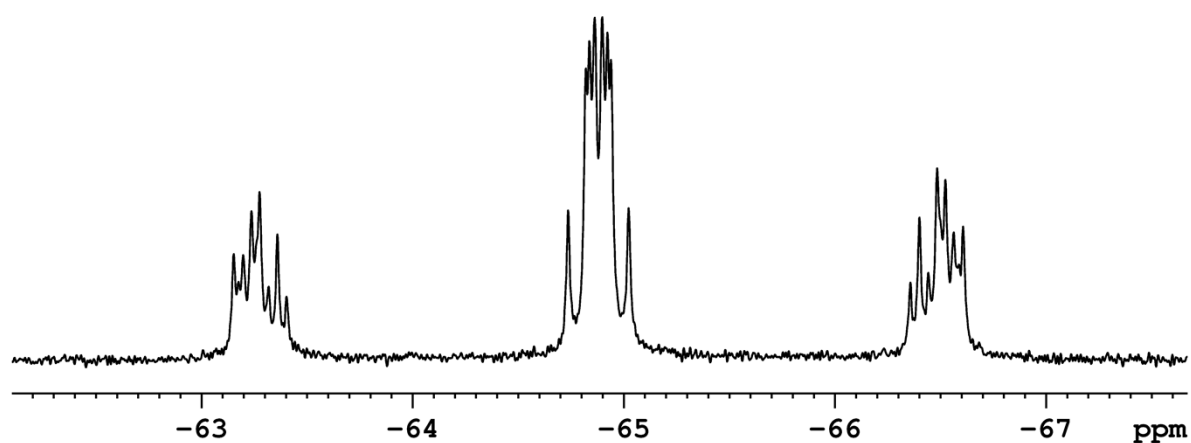


Figure S9. ^{31}P NMR spectrum of **2** in CD_2Cl_2 .

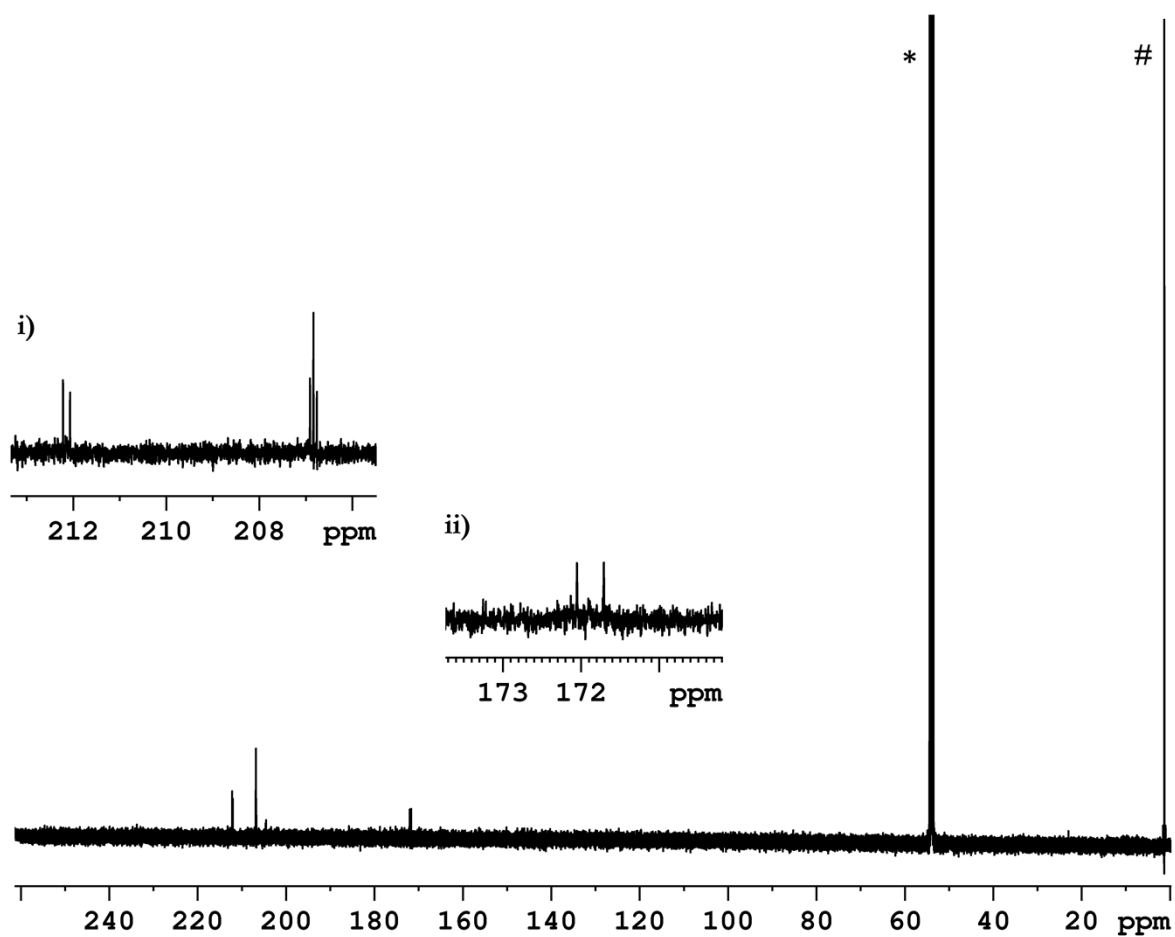


Figure S10. $^{13}\text{C}\{^1\text{H}\}$ NMR spectrum of **2** in CD_2Cl_2 . The resonance marked with * is to the solvent, and # is due to a grease impurity. Inset i) shows the zoomed in region for the molybdenum carbonyls, and inset ii) shows the phosphinecarboxamide resonance.

4. IR spectra

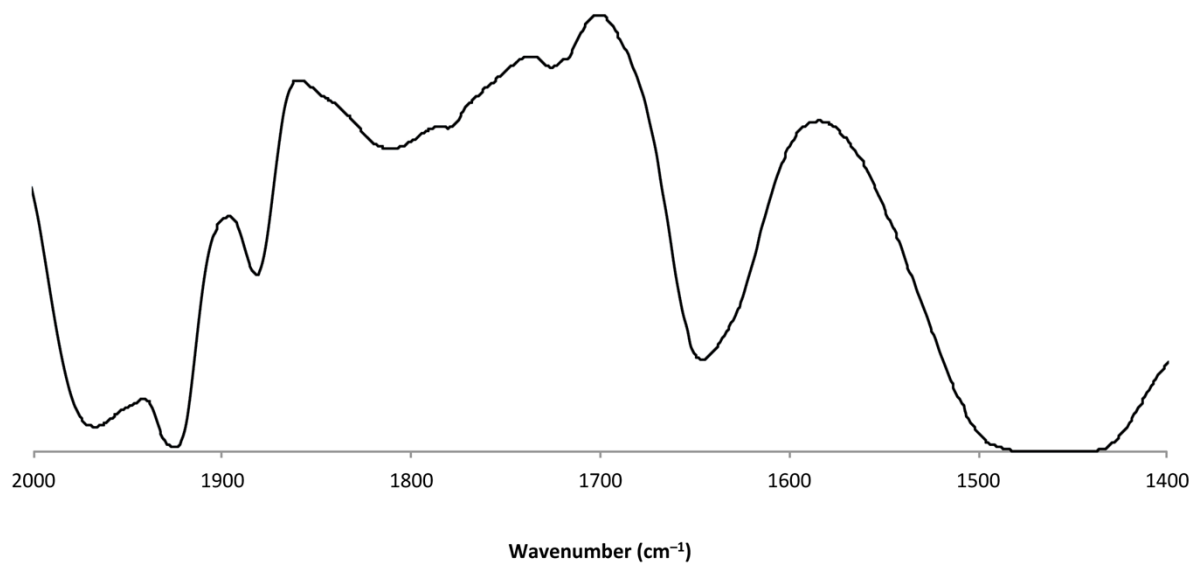


Figure S11. Dilute solution phase IR spectrum of **1** in THF, zoomed in to show the carbonyl region.

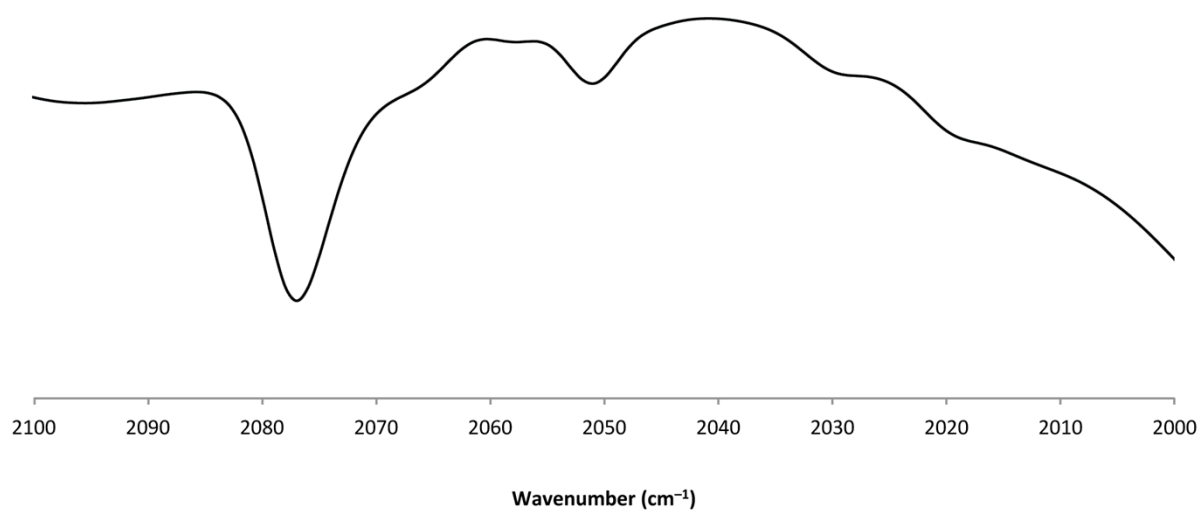


Figure S12. Concentrated solution phase IR spectrum of **1** in THF, zoomed in to show the pseudo-A₁ stretch at 2077 cm⁻¹.

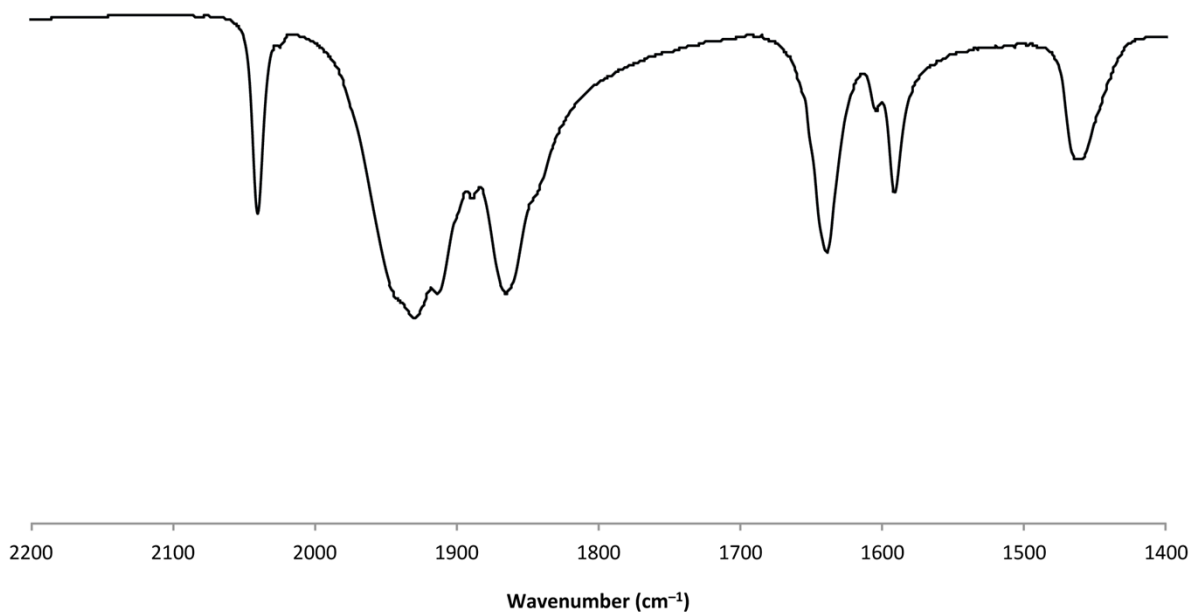


Figure S13. Solid state IR spectrum of **2**, zoomed in to show the carbonyl region.

5. References

- [1] D. Heift, Z. Benkő and H. Grützmacher, *Dalton Trans.* 2014, **43**, 831–840.
- [2] A. R. Jupp and J. M. Goicoechea, *Angew. Chem. Int. Ed.*, 2013, **52**, 10064–10067.
- [3] A. Tekkaya, C. Kayran, S. Ozkar and C. G. Kreiter, *Inorg. Chem.*, 1994, **33**, 2439–2443.
- [4] A. R. Jupp and J. M. Goicoechea, *J. Am. Chem. Soc.*, 2013, **135**, 19131–19134.
- [5] gNMR v5.0, Budzelaar, P. H. M., 1995-2006, IvorySoft.
- [6] J. Cosier and A. M. Glazer, *J. Appl. Crystallogr.*, 1986, **19**, 105–107.
- [7] *CrysAlisPro*, Agilent Technologies, Version 1.171.35.8.
- [8] (a) G. M. Sheldrick in *SHELXL97, Programs for Crystal Structure Analysis (Release 97-2)*, Institut für Anorganische Chemie der Universität, Tammanstrasse 4, D-3400 Göttingen, Germany, 1998. (b) G. M. Sheldrick, *Acta Crystallogr. Sect. A.*, 1990, **46**, 467–473. (c) G. M. Sheldrick, *Acta Crystallogr. Sect. A.*, 2008, **64**, 112–122.

- [9] (a) G. te Velde, F.M. Bickelhaupt, S. J. A. van Gisbergen, C. Fonseca Guerra, E. J. Baerends, J. G. Snijders and T. Ziegler, *J. Comp. Chem.*, 2001, **22**, 931–967. (b) C. Fonseca Guerra, J. G. Snijders, G. te Velde and E. J. Baerends, *Theor. Chem. Acc.*, 1998, **99**, 391–403. (c) ADF2013, SCM, Theoretical Chemistry, Vrije Universiteit, Amsterdam, The Netherlands, <http://www.scm.com>.
- [10] (a) A. D. Becke, *Phys. Rev. A*, 1988, **38**, 3098–3100. (b) J. P. Perdew and Y. Wang, *Phys. Rev. B*, 1986, **33**, 8822–8824.
- [11] S. Grimme, S. Ehrlich, and L. Goerigk, *J. Comp. Chem.*, 2011, **32**, 1456–1465.
- [12] E. van Lenthe, A. E. Ehlers and E. J. Baerends, *J. Chem. Phys.*, 1999, **110**, 8943–8953.
- [13] G. A. Zhurko, ChemCraft v1.7 (build 382); www.chemcraftprog.com.
- [14] J. P. Perdew and Y. Wang, *Phys. Rev. B*, 1992, **45**, 13244–13249.
- [15] J. P. Perdew, K. Burke and M. Ernzerhof, *Phys. Rev. Lett.*, 1996, **77**, 3865–3868.